RSC Advances

High performance Li4Ti5O12/CN anode material promoted by melamine-formaldehyde resin as carbon-nitrogen precursor

Journal:	*RSC Advances*
Manuscript ID:	RA-ART-04-2015-006374.R1
Article Type:	Paper
Date Submitted by the Author:	31-May-2015
Complete List of Authors:	Ren, Yurong; School of Materials and Engineering, Changzhou University Lu, Peng; School of Materials and Engineering, Changzhou University Ding, Jianning; School of Materials and Engineering, Changzhou University Huang, Xiaobing; College of Chemistry and Chemical Engineering, Hunan University of Arts and Science Wang, Hai-Yan; School of Chemistry and Chemical Engineering, Central South University, Zhou, Shibiao; College of Chemistry and Chemical Engineering, Hunan University of Arts and Science Chen, Yuandao; College of Chemistry and Chemical Engineering, Hunan University of Arts and Science Liu, Beiping; College of Chemistry and Chemical Engineering, Hunan University of Arts and Science

RSC Advances

RSC Advances

Dynamic Article Links ►

Cite this: DOI: 10.1039/c0xx00000x

www.rsc.org/xxxxxx

Paper

High performance $Li_4Ti_5O_{12}$/CN anode material promoted by melamine-formaldehyde resin as carbon-nitrogen precursor

Yurong Ren [a], Peng Lu [a] , Jianning Ding [a], Xiaobing Huang [b, c,*], Haiyan Wang [d], Shibiao Zhou [b,*], Yuandao Chen [b], Beijing Liu [b]

Received (in XXX, XXX) Xth XXXXXXXXX XXXX, Accepted Xth XXXXXXXXX XXXX
DOI: 10.1039/b000000x

Carbon-nitrogen coating approach using melamine-formaldehyde resin as carbon-nitrogen source is introduced in this work with the aim of getting high rate $Li_4Ti_5O_{12}$/CN composite. $Li_4Ti_5O_{12}$/CN composite, particle size of 50-100 nm in diameter, is well dispersed and the carbon-nitrogen layers are 2 nm in thickness. The composite delivers much higher electrochemical performance than those of $Li_4Ti_5O_{12}$. At 0.2 C and 10 C, it exhibits a discharge capacity of 172 mAh g^{-1} and 160 mAh g^{-1}, respectively, and after 250 cycles at 10 C, 97.4 % of its initial capacity is retained. The superior electrochemical performance can be attributed to the improved ionic and electronic conductivity in the electrode due to the uniform and ultrthin carbon-nitrogen coating layer.

1. Introduction

Rechargeable lithium ion batteries (LIBs) have long been considered to be one of the most promising energy storage systems because of the higher energy density, higher rate, higher stability, longer cycle life, and improved safety than competing batteries[1-3]. Currently commercial LIB usually uses graphite as anode, but a stable solid electrolyte interface (SEI) film formed on the surface of graphite/carbon particles and volume expansion/contraction during Li-ion intercalation/extraction could possibly cause serious safety problems[3-6].Therefore, it is highly desired to explore new anode materials with high safety and excellent cyclability instead of unsafe carbon material[7]. As one of the most excellent lithium ion battery anode materials, $Li_4Ti_5O_{12}$ has been extensively studied, owing to its particular advantages of low toxicity, low cost, easy preparation and low-strain lithium intercalation/desintercalation[8]. Furthermore, it possesses a flat voltage plateau at approximate 1.55 V (vs. Li^+/Li), which is higher than the reduction potential of most organic electrolytes, thus avoiding the formation of a solid-electrolyte interface (SEI) [6]. Nevertheless, the high rate performance of $Li_4Ti_5O_{12}$ is hindered by inherently poor electronic conductivity, which has been a main obstacle to its applications[9-10]. Several strategies have been proposed to solve this issue, including synthesizing the nanosized particles via various methods[7, 11, 12] and surface modification by means of conductive matters (Au, Ag, Cu, carbon, etc)[1,9,13,14]. In addition, cation doping in Li and Ti sites is another way to improve the electronic conductivity of $Li_4Ti_5O_{12}$, such as Na^+ [5], Ni^{2+} [15], Zn^{2+} [16], Al^{3+} [17], W^{6+} [18], Sr^{2+} [19]. Among them, synthesis of $Li_4Ti_5O_{12}$ with carbon has been demonstrated to effectively improve its electronic conductivity.

In an earlier study, it was found that the selected carbon precursors directly affect the characteristics of the carbon additive, in terms of its structure, distribution and thickness of carbon coating layer, which are proportional to the performance of C-coated composite electrode [20-23]. Doeff et al. found that the increased sp^2 coordinated carbon promised better electrochemical performance for $LiFePO_4$ [24-25]. Functionalized aromatic or ring-forming organic precursor has received considerable attention as carbon source for electrode materials [20,24,26]. As reported recently, the co-modifying of C&N can also induce the formation of conductive coating materials (CN_x) on the surface, which can efficiently enhance the surface conductivity and the electrical contact in the electrode [27]. To date, $Li_4Ti_5O_{12}$/CN composite with various carbon-nitrogen sources such as NH_3 and sugar [28], acetyl glucosamine [29] have been reported successively. With the consideration of functionalized aromatic or ring-forming carbon-nitrogen precursors, new carbon-nitrogen sources still need to be studied.

In this paper, we exploited a facile route to prepare carbon-nitrogen coated $Li_4Ti_5O_{12}$ composite by using functionalized aromatic melamine-formaldehyde resin as carbon-nitrogen precursor. For comparison, the pristine $Li_4Ti_5O_{12}$ without carbon-nitrogen coating was also synthesized.

2. Experimental

A stoichiometric amount of Li_2CO_3 (99.5%) and TiO_2 (99.5%) were dispersed in acetone with thoroughly ball-milling to form a slurry mixture. The obtained slurry was dried at 70 ◦C in a vacuum oven for 2 h. The resulting powder was heated in a horizontal quartz tube oven under flowing argon gas at 750 ◦C for 8 h to obtain the final $Li_4Ti_5O_{12}$. The synthesis of $Li_4Ti_5O_{12}$/CN composite was similar to that of $Li_4Ti_5O_{12}$, with melamine-formaldehyde resin mixed with raw materials in acetone.

Melamine-formaldehyde resin was also heated in a horizontal quartz tube oven under flowing argon gas, at 750 ◦C for 8 h to obtain the pyrolyzed carbon-nitrogen.

X-ray diffraction (XRD) data were examined by X-ray diffractometer (DX-2700, Dandong Haoyuan) utilizing a Cu-Ka1 source. Morphological studies were conductedby scanning electron microscope (SEM, JSM-6510LA) and transmission electron microscopy (TEM, JEOL JEM-2100F). X-ray photoelectron spectroscopy (XPS) measurement was performed on a K-Alpha1063 spectrometer. Thermal gravimetry (TG) was carried out with a NETZSCH STA 449C differential scanning

calorimeter under N_2 atmosphere at a ramping rate of 10 ◦C min. The BET surface area of the samples was detected by nitrogen adsorption–desorption at -196 ◦C using a Builder SSA-4200 apparatus. Four-point probe method (RTS-9, Guangzhou) was employed to measure the electronic conductivity.

Working electrodes were constructed by mixing the active material, Super-P carbon and LA-132 in the weight ratio of 85:10:5. Water was used as solvent. The slurry was cast onto Al foil using the Doctor-Blade technique and dried at 100 ◦C for 10 h in a vacuum oven. Finally, CR2032 coin-type cells were assembled in an argon-filled glove box, using lithium foil as the counter electrode, Celgard 2400 as the separator, and 1 mol/L $LiPF_6$ dissolved in a mixture of EC, DEC, DMC with a volume ratio of 1:1:1 as the electrolyte. Galvanostatic charge and discharge measurements were performed in a potential range of 1-3 V at room temperature. The AC impedance data were recorded in the frequency range 10^{-2} Hz to 10^5 Hz using CHI600E electrochemical station (Shanghai Chenhua).

3. Results and discussion

Fig. 1 presents the XRD patterns of the as-obtained $Li_4Ti_5O_{12}$ samples. As can be seen, both samples demonstrate the similar XRD patterns, which are well indexed to $Li_4Ti_5O_{12}$ phase with cubic spinel structure (Fd-3m space group). It is remarkable to note that the addition of melamine-formaldehyde resin has no effect on the crystal structure of spinel $Li_4Ti_5O_{12}$. Besides, there is no obvious carbon detected in the XRD pattern, which is most likely due to the low content and/or the amorphous structure of carbon [29]. Furthermore, the $Li_4Ti_5O_{12}$ shows a relatively sharp peak with high intensity. On the other hand, the $Li_4Ti_5O_{12}$/CN composite indicates the decreasing intensity of the peaks and broadening diffraction peaks. The above results suggest that the $Li_4Ti_5O_{12}$/CN composite probably have smaller crystallite size. It is well accepted that the presence of carbon-nitrogen could hinder the growth of $Li_4Ti_5O_{12}$ particles during the calcination process, which would result in the smaller crystallite size.

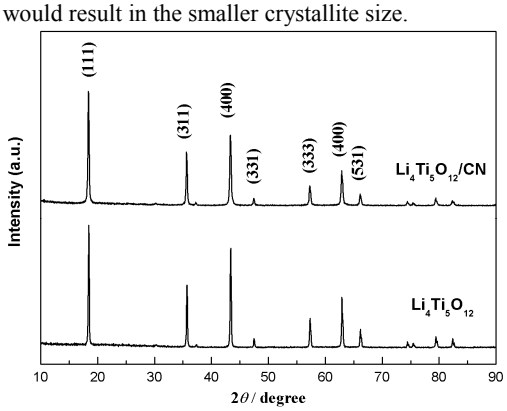

Fig. 1 XRD profiles of as-obtained $Li_4Ti_5O_{12}$ samples

Fig. 2 shows XRD patterns of carbon-nitrogen produced by pyrolysis of melamine-formaldehyde resin. As observed, the graphite peak at 2θ = 26° is high, which indicates that melamine-formaldehyde resin is favorable to form more highly graphitized carbons during the heat treatment process.

Important information on the surface electronic state of $Li_4Ti_5O_{12}$ and $Li_4Ti_5O_{12}$/CN composite is provided by XPS (Fig. 3a). It can be clearly to see that a new peak at around 399 eV ascribed to N 1s was appeared in $Li_4Ti_5O_{12}$/CN composite, while it cannot be detected for pure $Li_4Ti_5O_{12}$, demonstrating the presence of N in $Li_4Ti_5O_{12}$/CN composite [29]. It is worth noting that the atomic ratio of N/C is 13.3 % for $Li_4Ti_5O_{12}$/CN composite according to the peak area ratio of N1s to C1s. The high resolution XPS of N1s is displayed in Fig. 3b. Peaks around 398 eV and 400 eV are ascribed to C-N and C=N, respectively. These evidences clarify that the coating layer consists of N-doped carbon with at least two bonding ways between C and N atoms [29]. According to the recent report [29], the appearance of the C-N and C=N could lead to defects in the graphite structure and the existence of defects introduced by N doping would be beneficial to Li^+ diffusion in the interface. The high-resolution Ti2p of $Li_4Ti_5O_{12}$/CN is shown in Fig. 3c. Two broad peaks centered around 464.5 and 458.6 eV are well in accordance with the characteristic peaks of Ti 2p1/2 and Ti 2p3/2 of Ti^{4+} in the $Li_4Ti_5O_{12}$/CN composite [27]. Compared to the Ref reported by Ming et al [27], the two extra peaks appeared at ~462.0 and ~457.6 eV that attributed to Ti2p1/2 and Ti2p3/2 peaks of Ti^{3+} were not observed. This means that the Ti^{3+} sites were not successful introduced in $Li_4Ti_5O_{12}$/CN composite during the calcination under the reduction ability of C&N. To determine the amount of CN in the composite of $Li_4Ti_5O_{12}$/CN, TG test of as-prepared material was carried out (Fig. 4). It can be clearly to see that the content of CN in the composite of $Li_4Ti_5O_{12}$/CN is 2.5 % by weight. Based on the XPS and TG results, the content of N in the composite of $Li_4Ti_5O_{12}$/CN is calculated to be 0.8%.

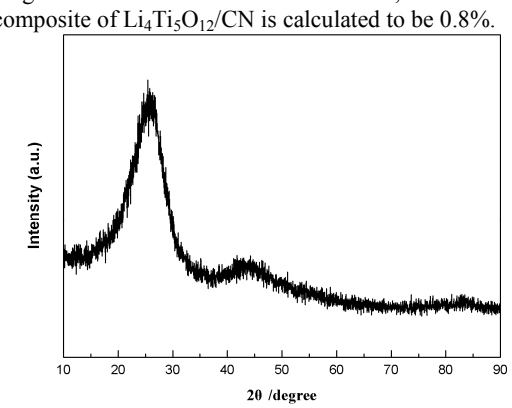

Fig 2 XRD profile of carbon-nitrogen produced by pyrolysis of melamine-formaldehyde resin

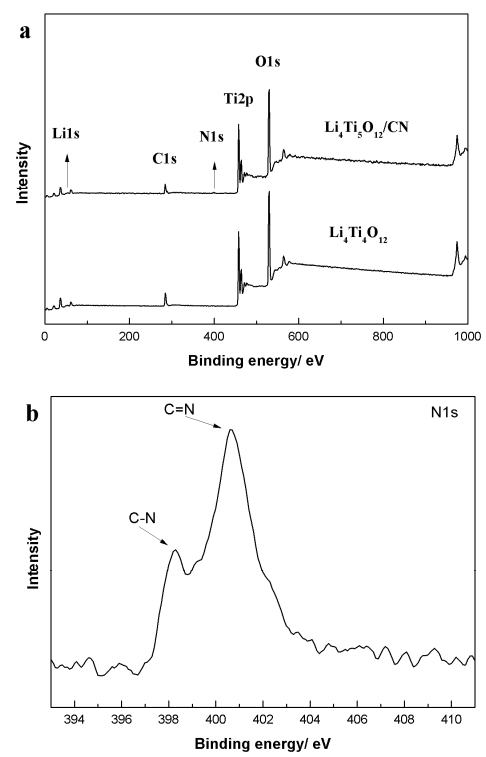

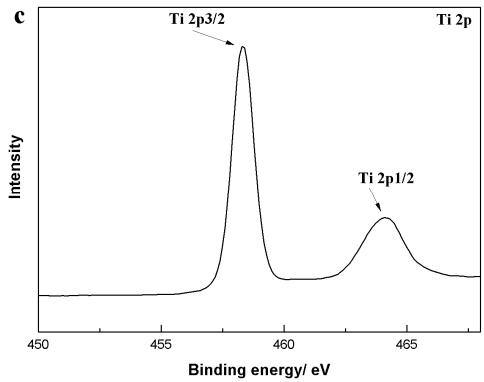

Fig.3.XPS survey spectrums of $Li_4Ti_5O_{12}$ and $Li_4Ti_5O_{12}$/CN composite (a), typical high-resolution XPS spectra of N1s for $Li_4Ti_5O_{12}$/CN composite (b) and typical high-resolution XPS spectra of Ti 2p1/2 and Ti 2p3/2 for $Li_4Ti_5O_{12}$/CN composite (c)

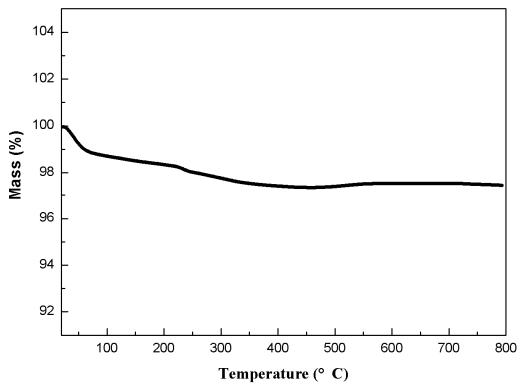

Fig. 4. TG curve of $Li_4Ti_5O_{12}$/CN composite

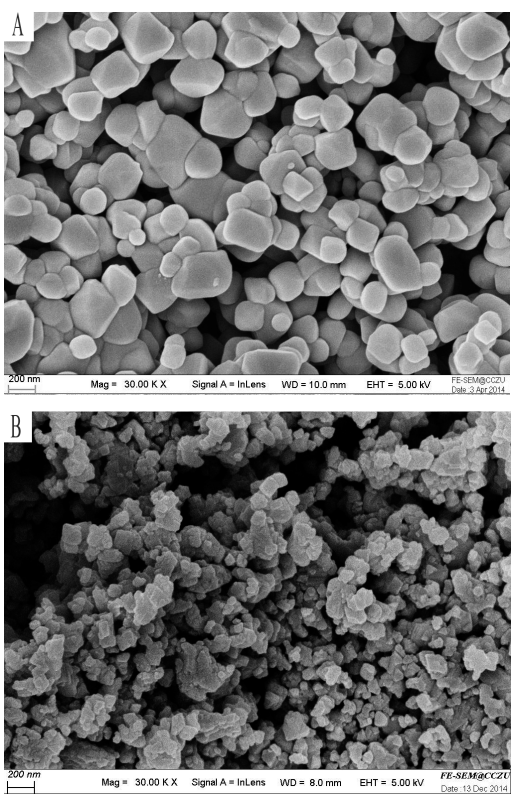

Fig. 5 SEM images of the samples: (A) $Li_4Ti_5O_{12}$; (B) $Li_4Ti_5O_{12}$/CN composite

Fig. 5 shows the SEM images of the as-received $Li_4Ti_5O_{12}$ and $Li_4Ti_5O_{12}$/CN composite. Clearly, the $Li_4Ti_5O_{12}$ has as larger particles as 100-400 nm in diameter, whereas the $Li_4Ti_5O_{12}$/CN has a smaller particle size of 50-100 nm in diameter. Both XRD and SEM results reveal that carbon-nitrogen coating via the pyrolysis of melamine-formaldehyde resin plays an important role in controlling the growth of particles. The reduced particle size results in shortening of the diffusion path of Li^{+} [30] and hence better electrochemical performance of $Li_4Ti_5O_{12}$/CN compared to that of $Li_4Ti_5O_{12}$. This is further supported by the electrochemical measurements described below. The data from the BET measurement shown in Table1, gives a specific surface area of about 6.2 and 14.8m^2 g^{-1} for the crystalline material from $Li_4Ti_5O_{12}$ and $Li_4Ti_5O_{12}$/CN composite, respectively. Apparently, the smaller particles of $Li_4Ti_5O_{12}$/CN composite promise larger specific surface area, resulting in short lithium ion diffusion path and enough contact between the active material and electrolyte, thus leading to the enhancement of electrochemical performance of $Li_4Ti_5O_{12}$/CN.

Table 1 Table 1 BET surface area of both samples

Samples	BET surface area (m^2 g^{-1})
$Li_4Ti_5O_{12}$	6.2
$Li_4Ti_5O_{12}$/CN	14.8

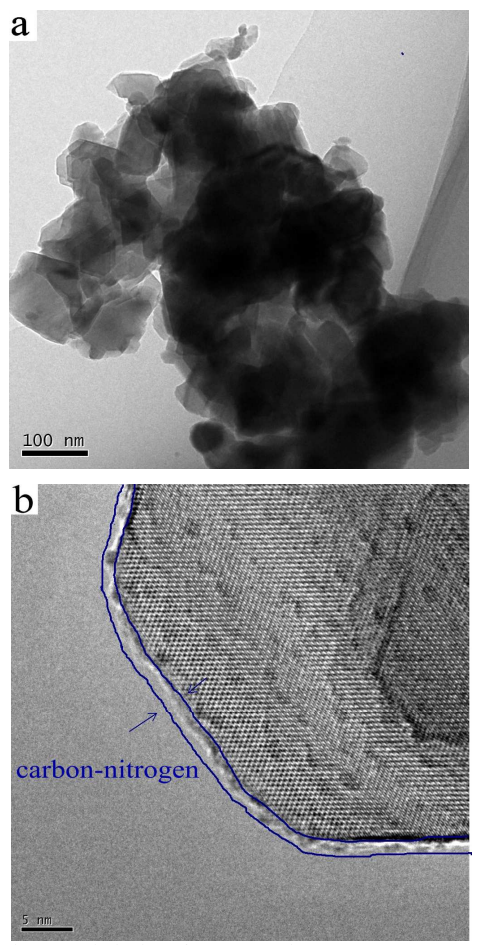

Fig. 6 TEM images of $Li_4Ti_5O_{12}$/CN composite

The morphology of $Li_4Ti_5O_{12}$/CN composite was further investigated by HRTEM, which is shown in Fig. 6. It can be seen that $Li_4Ti_5O_{12}$/CN composite exhibits well distributed fine particles (50-100 nm), which is in good agreement with above result in SEM image. It is worth noting that a very thin and

uniform carbon -nitrogen layer with the thickness of 2 nm is clearly seen on the surface of $Li_4Ti_5O_{12}$ particle from Fig. 6b.

Fig. 7 shows the charge and discharge profiles of $Li_4Ti_5O_{12}$ and $Li_4Ti_5O_{12}$/CN electrodes at 0.2 C for the first cycle and in the voltage range from 1 V to 3 V. Each sample shows a flat plateaus around 1.5-1.6 V (versus Li^+/Li), which corresponds to the reversible phase transition between $Li_4Ti_5O_{12}$ and $Li_7Ti_5O_{12}$ [31]. Furthermore, the potential difference between the charge and discharge plateau of the $Li_4Ti_5O_{12}$/CN composite is smaller than that of the $Li_4Ti_5O_{12}$. It suggests smaller electrode resistance and excellent transport properties of $Li_4Ti_5O_{12}$/CN composite which comes from the layer of the pyrocarbon-nitrogen present on the $Li_4Ti_5O_{12}$ particle surface, providing a good electronic contact between the particles and lead to minimized kinetic polarization[32]. In addition, $Li_4Ti_5O_{12}$/CN composite exhibited a higher initial coulombic efficiency (98.9%) than that of pure $Li_4Ti_5O_{12}$ (97.2%), which is due to the presence of a thin carbon-nitrogen layer [33].

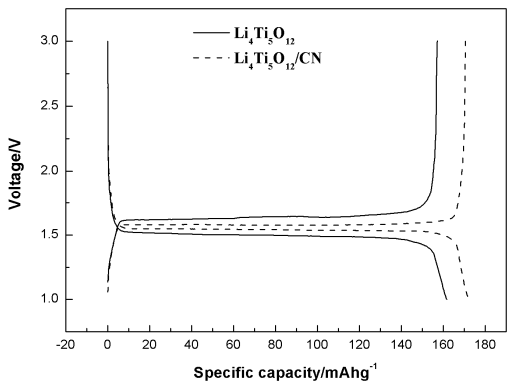

Fig. 7 The first charge and discharge curves for $Li_4Ti_5O_{12}$ and $Li_4Ti_5O_{12}$/CN composite

To examine the effect of carbon-nitrogen coating in improving the rate capability, we investigated the specific capacity of $Li_4Ti_5O_{12}$ and $Li_4Ti_5O_{12}$/CN under various current rates and the result is plotted in Fig. 8. It is clear that the discharge capacities of both samples gradually decrease with the increasing of the rate. This is because the utilization of the active material decreases as the rate increases [34]. However, $Li_4Ti_5O_{12}$/CN composite manifested a higher discharge capacity than $Li_4Ti_5O_{12}$, which is more and more obvious with the current densities increasing. For instance, at 0.2 C and 10 C, the discharge capacity of $Li_4Ti_5O_{12}$/CN composite remained 172 mAh g^{-1} and 160 mAh g^{-1}, respectively, while the discharge capacity of $Li_4Ti_5O_{12}$ remained only 161 mAh g^{-1} and 80 mAh g^{-1}. Obviously, $Li_4Ti_5O_{12}$/CN composite exhibits much better rate capacity than $Li_4Ti_5O_{12}$. Long-term cycling stability of $Li_4Ti_5O_{12}$/CN composite was investigated at a current rate of 10 C for another 250 cycles after the 10 cycles at 0.2 C (Fig.9). As illustrated, the initial discharge capacity of $Li_4Ti_5O_{12}$/C composite is 160 mAh g^{-1}, and 97.4 % of the initial discharge capacity after 250 cycles is retained. To our knowledge, $Li_4Ti_5O_{12}$/CN composite exhibits the best rate capability and cycling stability among those carbon-nitrogen sources reports so far. Zhang et al [28] reported $Li_4Ti_5O_{12}$/CN composite with NH_3 and sugar as carbon-nitrogen source delivered a discharge capacity of 138 mAh g^{-1} and 125 mAh g^{-1} at 6C, 12C, respectively. Li et al [29] prepared nitrogen-doped carbon coated $Li_4Ti_5O_{12}$ using acetyl glucosamine as carbon-nitrogen source showed a discharge capacity of 167mAh g^{-1} at 0.2 C, however, it decreased to 133 mAh g^{-1} at 10 C. The superior rate performance of $Li_4Ti_5O_{12}$/CN composite in this work should be resulted from the following reasons: (1) the appearance of the C-N and C=N in carbon coating layer (see in Fig. 3b) could lead to defects in the graphite structure and the existence of defects introduced by N doping would be beneficial to Li^+ diffusion in the interface [27]; (2) Much highly graphitized carbons obtained during pyrolysis of functionalized aromatic melamine-formaldehyde resin (see in Fig. 2) ensures good electronic conductivity [22]; (3) In-situ coating approach allows the thin and homogeneous layers on the surface of $Li_4Ti_5O_{12}$ and keeps the larger specific surface area and smaller particle size, resulting in short lithium ion diffusion path and enough contact between the active material and electrolyte.

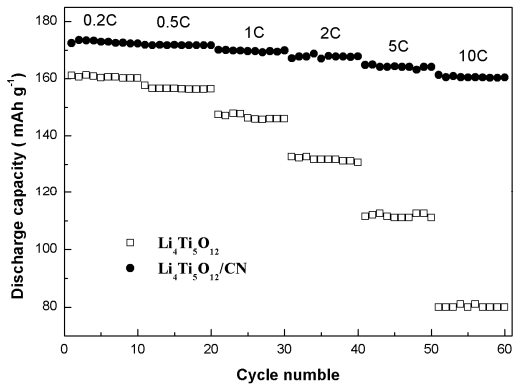

Fig. 8 Cyclic performance of the $Li_4Ti_5O_{12}$ and $Li_4Ti_5O_{12}$/CN composite at different rates

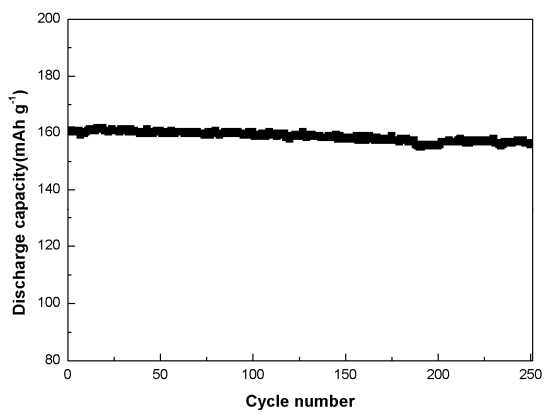

Fig. 9 Cycle performance of $Li_4Ti_5O_{12}$/CN composites at 10 C

Fig. 10 gives the impedance spectra of the $Li_4Ti_5O_{12}$ and $Li_4Ti_5O_{12}$/CN electrodes measured at the stable voltage of 1.55 V, respectively. It is obvious that each Nyquist plot is composed of a depressed semicircle and a straight line. According to the literature [5, 35-36], the intercept at the *Z'* axis in the high frequency corresponds to the ohmic resistance (R_e), representing the resistance of the electrolyte. The semicircle in the middle frequency range is attributed to the charge transfer resistance (R_{ct}). The straight line in the low frequency is associated with lithium ion diffusion in $Li_4Ti_5O_{12}$, The lithium ion diffusion coefficient could be calculated from the low frequency plots according to the following equation [37-41]:

$$D = R^2T^2 / 2A^2n^4F^4C^2\sigma^2 \qquad (1)$$

Where R is the gas constant, T is the absolute temperature, A is the surface areaof the cathode, n is the number of electrons per molecule during oxidation, F is theFaraday constant, C is the concentration of lithium ion, σ is the Warburg factor which is relative with Z_{re} [37-41].

$$Z_{re} = R_D + R_L + \sigma\omega^{-1/2} \qquad (2)$$

Where ω is frequency. The relationships between Z_{re} and the reciprocal square root of frequency in the low frequency are shown in Fig. 11. All the parameters obtained and calculated from EIS are summarized in Table 2. As can be seen, $Li_4Ti_5O_{12}$/C

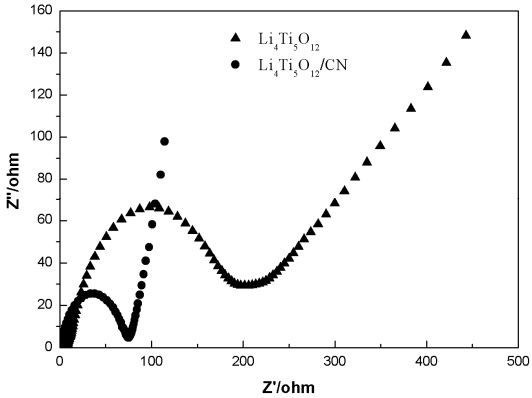

Fig. 10 Nyquist plots of the $Li_4Ti_5O_{12}$ and $Li_4Ti_5O_{12}$/CN electrodes

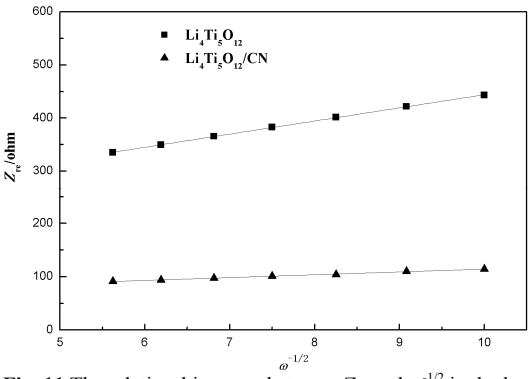

Fig. 11 The relationship curve between Z_{re} and $\omega^{-1/2}$ in the low frequency

Table 2 Impedance parameters of the $Li_4Ti_5O_{12}$ and $Li_4Ti_5O_{12}$/CN composite

Samples	R_e (Ω)	R_{ct} (Ω)	σ(Ω $s^{-1/2}$)	D (cm^2 s^{-1})
$Li_4Ti_5O_{12}$	4.3	202	24.7	6.11×10^{-11}
$Li_4Ti_5O_{12}$/CN	1.7	75	5.3	1.33×10^{-9}

-N composite exhibits the smaller charge-transfer resistance and higher lithium diffusion coefficient than those of $Li_4Ti_5O_{12}$. $Li_4Ti_5O_{12}$ and $Li_4Ti_5O_{12}$/CN composite were pressed into disk-shaped pellets and their electronic conductivity measured by the four-point dc method. Table 3 presents a comparison of conductivity for $Li_4Ti_5O_{12}$ and $Li_4Ti_5O_{12}$/CN composite . As can be seen, the conductivity of $Li_4Ti_5O_{12}$/CN composite (1.27×10^{-2} S cm^{-1}) is much higher than that of $Li_4Ti_5O_{12}$ (8.89×10^{-5} S cm^{-1}). The above results suggest that $Li_4Ti_5O_{12}$/CN composite by using functionalized aromatic melamine-formaldehyde resin as carbon-nitrogen precursor is favorable to improve the electrical conductivity and ionic conductivity, yielding superior rate properties.

Table 3 Electronic conductivity of the samples

Samples	Electronic conductivity(S cm^{-1})
$Li_4Ti_5O_{12}$	8.89×10^{-5}
$Li_4Ti_5O_{12}$/CN	1.27×10^{-2}

4.Conclusion

In summary, melamine-formaldehyde resin as carbon-nitrogen source was proposed for the first time to improve the electrochemical performance of $Li_4Ti_5O_{12}$. $Li_4Ti_5O_{12}$/CN composite exhibited much better electrochemical performance. It delivers a discharge capacity of 160 mAh g^{-1} at 10 C, and after 250 cycles, 97.4 % of its initial capacity is retained. It is believed that much highly graphitized nitrogen-doped carbons obtained during pyrolysis of functionalized aromatic melamine-formaldehyde resin assures the high conductivity. Furthermore, carbon-nitrogen layer coated on the surface of $Li_4Ti_5O_{12}$ favors the formation of $Li_4Ti_5O_{12}$ with the smaller particle size and larger specific surface area, which could shorten the diffusion path of lithium ion and further expedite the ion transferring. This strategy could pave a new way for $Li_4Ti_5O_{12}$ and other electrode materials to achieve the significant improvement of electrochemical properties.

Acknowledgments

This project was financially supported by the National Nature Science Foundation of China (No. 51304077), the Hunan Provincial Natural Science Foundation of China (No. 13JJ4100 and 12JJ8004), the Construct Program of the Key Discipline in Hunan Province of China (Applied Chemistry), the Opening Project of Material Corrosion and Protection Key Laboratory of Sichuan Province of China (No.2013CL12, 2014CL03 and 2014CL15), the State Key Laboratory of Alternate Electrical Power System with Renewable Energy Sources (No. LAPS15001).

Notes and references

[a] *School of Materials and Engineering, Changzhou University, Jiangsu 213164, China*
[b] *College of Chemistry and Chemical Engineering, Hunan University of Arts and Science, Changde 415000, China*, Tel.:+86137626812796. *E-mail:* hxb220170@yahoo.com(X.B. Huang) , zsb201@126.com(S.B. Zhou)
[c] *Material Corrosion and Protection Key Laboratory of Sichuan Province, Zigong 643000, China*
[d] *College of Chemistry and Chemical Engineering, Central South University, Changsha 410083, China*

1. W. Wang, Y.Y Guo , L. X. Liu, S. X. Wang, X. J. Yang, H. Guo, J. Power Sources 245 (2014) 624-629.
2. S. S. Tao, W. B. Yue, M. Y. Zhong, Z. J. Chen, Yu Ren, Appl. Mater. Interfaces 6 (2014) 6332−6339.
3.S. Yang, W. B. Yue, J. Zhu , Y. Ren, X. J. Yang, Adv. Funct. Mater. 23 (2013)3570-3576.
4.Y. Wang, H. B. Rong, B. Z. Li, L. D. Xing, X. P. Li, W.S. Li, J. Power Sources 246 (2014) 213-218.
5. T. F. Yi, S. Y. Yang, X. Y. Li, J. H. Yao, Y. R. Zhu, R. S. Zhu, J. Power Sources 246 (2014) 505-511.
6. C. M. Zhang, Y. Y. Zhang, J. Wang, D. Wang, D. N. He, Y. Y. Xia, J. Power Sources 236 (2013) 118-125.
7. X. R. Li, H. Hua, S. Huang, G. G. Yu, L. Gao, H. W. Liu, Y. Yu, Electrochim. Acta 112 (2013) 356-363
8. C. Jamin, K. Traina, D. Eskenazi, N. Krins, R. Cloots, B. Vertruyen, F. Boschini, Mater. Res. Bull. 48(2013) 4641-4646.
9. Z. J. He, Z. X. Wang, L. Cheng, T. Li, X. H. Li, H. J. Guo, F. X. Wu, Mater. Lett. 107 (2013)273-275
10. W. Fang, X.Q. Cheng, P.J. Zuo, Y.L. Ma, G.P. Yin, Electrochim. Acta 93 (2013)173-178.
11. H. J. Luo, L. F. Shen, K. Rui, H. S. Li, X.G. Zhang, J. Alloys Compd. 572 (2013) 37-42.

12. H. F. Ni, L. Z. Fan, J. Power Sources 214 (2012)195-199.
13. M. Krajewski, M. Michalska, B. Hamankiewicz, D. Ziolkowska, K. P. Korona, J. B. Jasinski, M. Kaminska, L. Lipinska, A. Czerwinski, J. Power Sources 245 (2014)764-771.
14. X. B. Hu, Z. J. Lin, K. R. Yang, Y. J. Huai, Z. H. Deng, Electrochim. Acta 56 (2011) 5046-5053.
15. C. F. Lin, M. O. Lai, L. Lu, H. H. Zhou, Y. L. Xin, J. Power Sources 244(2013) 272-279.
16. Z. W. Zhang, L. Y. Cao, J. F. Huang, S. Zhou, Y. C. Huang, Y. J. Cai, Ceram. Int. 39 (2013) 6139-6143.
17. J. Y. Lin, C. C. Hsu, H. P. Ho, S. H. Wu, Electrochim. Acta 87 (2013) 126-132.
18. Q. Y. Zhang, C. L. Zhang, B. Li, D. D. Jiang, S. F. Kang, X. Li, Y. G. Wang, Electrochim. Acta 107 (2013)139-146.
19. H. B. Wu, S. Chang, X. L. Liu, L. Q. Yu, G. L. Wang, D. X. Cao, Y. M. Zhang, B. F .Yang, P. L. She, Solid State Ionics 232(2013)13-18.
20. Z. Y. Chen, H. L. Zhu, S. Ji, R. Fakir, V. Linkov, Solid State Ionics 179 (2008) 1810-1815.
21. Y. D. Cho, G. T. K. Fey, H. M. Kao, J. Power Sources 189 (2009) 256-262.
22. J. D. Wilcox, M. M. Doeff, M. Marcinek, R. Kostecki, J. Electrochem. Soc. 154 (2007) A389-A395.
23. X. Zhi, G. Liang, L. Wang, X. Ou, L. Gao, X. Jie, J. Alloys Compd. 503 (2010) 370-374.
24. M. M. Doeff, Y. Q. Hu, F. Mclarnon, R. Kostecki, Electrochem. Solid-State Lett. 6 (2003) A207-A209.
25. Y. Q. Hu, M. M. Doeff, R. Kostecki, R. Finones, J. Electrochem. Soc. 151 (2004)A1279-A1285.
26. H. M .Xie, R. S. Wang, J. R. Ying, L. Y. Zhang, A. F. Jalbout, H. Y. Yu, G. L. Yang, X. M. Pan, Z. M. Su, Adv. Mater. 18 (2006) 2609-2613.
27. H. Ming, J. Ming, X. W. Li, Q. Zhou, H. H. Wang, L. L. Jin, Y. Fu, J. Adkins, J. W. Zheng, Electrochim. Acta 116(2014)224-229.
28. H. Q. Zhang, Q. J. Deng, C. X. Mou, Z. L. Huang, Y. Wang, A. J. Zhou, J. Z. Li, J. Power Sources 239 (2013) 538-545.
29. H. S. Li, L. F. Shen, X. G. Zhang, J. Wang, P. Nie, Q. Che, B. Ding, J. Power Sources 221 (2013) 122-127.
30. E. Avci, M. Mazman, D. Uzun, E. Biçer, T. Sener, J. Power Sources 240 (2013) 328-337.
31. T. F. Yi, Y. Xie, Q. J. Wu, H. P. Liu, L. J. Jiang, M. F. Ye, R. S. Zhu, J. Power Sources 214 (2012) 220-226.
32. J.L. Li, T. Suzuki, K. Naga,Y. Ohzawa, T. Nakajima, Mater. Sci. Eng. B 142 (2007) 86-92
33. Z. H. Bi, M. P. Paranthaman, B. K. Guo, R. R. Unocic, H. M. Meyer, C. A. Bridges, X. G. Sun, S. Dai, J. Mater. Chem. A 2 (2014) 1818-1824
34. X. H. Liu, Z.W. Zhao, Powder Technol. 197(2010)309-313.
35. D. Sun, H. Y. Wang, P. Ding, N. Zhou, X. B. Huang, S. Tan, Y. G. Tang, J. Power Sources 242 (2013) 865-871.
36. H. Y. Wang, T. L. Hou, D. Sun, X. B. Huang, H. N. He, Y. G. Tang, Y. N. Liu, J. Power Sources 247 (2014) 497-502.
37. D. Sun, G. H. Jin, H. Y. Wang, P. Liu, Y. Ren, Y. F. Jiang, Y. G. Tang, X. B. Huang, J. Mater. Chem. A 2 (2014) 12999-13005.
38. H. N. He, G. H. Jin, H. Y. Wang, X. H. Huang, Z. H. Chen, D. Sun, Y. G. Tang, J. Mater. Chem. A 2 (2014) 3563-3570.
39. D. Sun, G. H. Jin, H. Y. Wang, X. B. Huang, Y. Ren, J. C. Jiang, H. N. He, Y. G.Tang, J. Mater. Chem. A 2(2014)8009-8016.
40. A.Y. Shenouda, H.K. Liu, J. Alloys Compd. 447 (2009) 498-503.
41. A.Y. Shenouda, H.K. Liu, J. Power Sources 185 (2008) 1386-1391.
.